

A new way to produce green *p*-xylene: rapeseed oil conversion over HMFI/SiC catalytic material

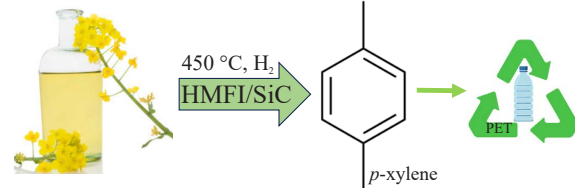
Alexey G. Dedov,^{a,b} Alexey S. Loktev,^{*,a,b} Alexander A. Karavaev,^{a,b}
Malika N. Vagapova^{a,b} and Kirill A. Cherednichenko^b

^a A. V. Topchiev Institute of Petrochemical Synthesis, Russian Academy of Sciences, 119991 Moscow, Russian Federation. E-mail: al57@rambler.ru

^b National University of Oil and Gas 'Gubkin University', 117917 Moscow, Russian Federation

DOI: 10.71267/mencom.7625

The conversion of rapeseed oil using a catalytic material containing HMFI zeolite and silicon carbide was studied for the first time. The synthesized material effectively catalyzes the conversion of rapeseed oil into liquid hydrocarbons that mostly contain aromatic hydrocarbons, including a mixture of isomeric xylenes, in which the *p*-xylene content reaches 75%.



Keywords: rapeseed oil, zeolite HMFI (ZSM-5), silicon carbide, hydrothermal microwave synthesis, green *p*-xylene, green hydrocarbons.

Production of petrochemicals from biomass, including vegetable oils, is consistent with the principles of green chemistry, the global low-carbon strategy and carbon cycling. Fatty acid triglycerides, the major component of vegetable oils, mainly contain esters of oleic, palmitic, stearic, linoleic and linolenic acids.¹ There are various approaches to the synthesis of biofuels and petrochemicals from vegetable oils: transesterification,^{2,3} hydroconversion,⁴ catcracking,^{5,6} pyrolysis,⁷ etc. Industrial technologies for vegetable oil processing generally based on two-stage processes developed by several leading companies. First, the hydrodeoxygenation and hydrodecarboxylation of oils are carried out over catalysts such as NiMo/Al₂O₃, CoMo/Al₂O₃, etc., then the hydroisomerization of intermediates proceeds over Pt, Pd, Ir and Re supported on zeolites or sulfonated oxide systems.⁸

One of the alternative approaches could be the one-step catalytic conversion of fatty acid triglycerides into hydrocarbons using catalysts based on Mordenite framework inverted (MFI) or Zeolite Socony Mobil (ZSM-5) zeolites. The resulting hydrocarbons, in addition to other components, generally contain a mixture of aromatic hydrocarbons, including *p*-xylene.

Along with other industrial applications, *p*-xylene is on large scale used for the synthesis of terephthalic acid and polyethylene terephthalate, a thermoplastic material that is employed in the manufacture of films, textile fibers, plastic tableware, etc.⁹

At present *p*-xylene is primarily produced from petroleum feedstocks *via* multistage separation of reforming naphtha products containing a fraction enriched in xylenes. The *m*- and *o*-xylenes obtained along with *p*-xylene can be isomerized to produce additional *p*-xylene. Inasmuch as the resulting equilibrium mixture of the three xylenes contains only *ca.* 24% *p*-xylene, the separation and isomerization steps have been repeated several times.¹⁰

Since the demand for *p*-xylene annually increases by an average of 6–8%,⁹ the urgent task is development of new technologies for its production, including the processing of renewable feedstocks.

MFI (ZSM-5) zeolites are used in various petrochemical processes, involving the renewable feedstocks processing. These zeolites possess the molecular sieve effect owing to the presence of an ordered 0.53 × 0.56 nm micropore system, acidic properties and high specific surface area. It was found,¹⁰ that in the pores of ZSM-5 the diffusion of *p*-xylene having a molecular diameter of 0.53 nm proceeds more effectively compared with *ortho*- and *meta*-xylenes possessing a larger molecular diameter. Therefore, the microporous structure of ZSM-5 zeolites can promote a more selective production of *p*-xylene from different feedstocks.

The direct one-stage conversion of rapeseed oil into hydrocarbons over materials containing non-promoted zeolite MFI (ZSM-5) has been the subject of a scarce number of publications. The hydroconversion of rapeseed oil on MFI/MCM-41 synthesized by the hydrothermal microwave method was studied.¹¹ The total yield of xylenes has not exceeded 4 wt%, the yields of isomeric xylenes are not given. This composition promoted by zinc and chromium also catalyzes the conversion of isobutanol into *p*-xylene containing hydrocarbon product, its yield reaches 7 wt%.¹²

The conversion of rapeseed oil over HZSM-5 (proton form of ZSM-5) at 400 °C has been reported earlier.¹³ The yield of the BTX (benzene–toluene–xylene) fraction was 40 wt% and the total yield of *m*- and *p*-xylenes reached 12 wt%.

Thus, the catalysts containing MFI zeolites allow one the synthesis of C₅₊ hydrocarbons, including aromatics and xylenes from various types of feedstocks. At the same time, petroleum feedstock is mainly used to obtain of *p*-xylene. The synthesis of *p*-xylene from a renewable feedstock, such as rapeseed oil, catalyzed by MFI zeolites is still insufficiently studied.

The microporous structure of MFI zeolites impedes the diffusion of a number of reagents. Coke deposition on the MFI surface also causes their deactivation, since it prevents the access of reagents to active centers located in the micropores. One of the approaches to solving these problems is to use the zeolite-containing materials with additional mesoporous structure, e.g., MFI and silicon carbide (SiC). The combination of MFI and

chemically inert mesoporous silicon carbide with high thermal conductivity could improve heat and mass transfer of material.^{14–16}

Here we describe a new one-step method for producing hydrocarbons, *p*-xylene in particular, *via* rapeseed oil conversion over the catalytic material containing HMFI zeolite (proton form of MFI zeolite) and silicon carbide introduced at the stage of HMFI synthesis. The catalyst was synthesized by the hydrothermal microwave method, that allowed the zeolite crystallization stage to be carried out in 3 h. This catalyst, designated as HMFI/SiC, enabled a marked increase in the content of *p*-xylene in the mixture of isomeric xylenes contained in the rapeseed oil conversion products. The technique of hydrothermal microwave synthesis of the HMFI/SiC and its characterization by ICP-OES, XRD, SEM, low-temperature nitrogen sorption, ammonia thermodesorption and IR spectroscopy of adsorbed pyridine, were described in our previous publications^{14–17} (for details, see Online Supplementary Materials). The spent catalyst was studied by thermogravimetric analysis (TGA) and transmission electron microscopy (TEM).

The zeolite content in the HMFI/SiC calculated on the basis of the characteristic band intensities in its IR spectrum¹⁷ related to those for pure HMFI zeolite was 77%. These data are consistent with the XRD results (see Figure S1 in Online Supplementary Materials). Low-temperature nitrogen physisorption analysis of the HMFI/SiC¹⁷ showed $S_{\text{BET}} = 393 \text{ m}^2 \text{ g}^{-1}$, $V_{\text{micropores}} = 0.16 \text{ cm}^3 \text{ g}^{-1}$ and $V_{\text{mesopores}} = 0.06 \text{ cm}^3 \text{ g}^{-1}$.

According to the IR spectroscopy of adsorbed pyridine (Table S1), the zeolite component of the HMFI/SiC material synthesized with silicon carbide addition to the initial mixture contains more Brönsted and Lewis acid centers per g of the zeolite component than HMFI synthesized by a similar method without the addition of silicon carbide. This, pursuant to the data,¹⁸ can facilitate more intensive processes of cyclization and dehydrogenation of intermediate products of oil conversion to aromatic compounds.

ICP-OES studies showed that the synthesis of zeolite with the addition of silicon carbide can increase the content of aluminum ions in the crystal lattice of zeolite contained in HMFI/SiC, compared with the zeolite synthesized by the same method without silicon carbide (Table S2). An enhanced content of aluminum ions apparently contributes to an increase in the number of Brönsted and Lewis acid sites in the zeolite of the HMFI/SiC material in comparison with the zeolite containing no silicon carbide. It can be also assumed that higher amount of acidic centers may also be due to a more defective zeolite structure caused by crystallization in the presence of silicon carbide. It is possible that SiC is able to interact with the emerging MFI framework, thereby affecting the distribution of silicon and aluminum in the zeolite (*e.g.*, preventing the complete crystallization of the zeolite), thus contributing to the occurrence of defects in the resulting material. Therefore, presence of SiC can affect the local environment of zeolite lattice atoms, mainly Al, enhancing their ability to act as protons donors or electron pairs acceptors, thereby increasing the overall acidity.

NH₃-TPD data demonstrate that the HMFI/SiC is characterized by a relatively high total concentration of acid centers – 510 $\mu\text{mol g}^{-1}$. Of these, 204 mmol g^{-1} corresponds to the thermal desorption of ammonia at $T < 300^\circ\text{C}$ and 306 mmol g^{-1} corresponds to the thermal desorption of ammonia at $T > 300^\circ\text{C}$.

Rapeseed oil (Lebyazhsky plant of vegetable oils, Russia) was used as a feedstock; its fatty acid composition is presented in Table S3. Catalytic experiments on rapeseed oil conversion were run in a quartz flow reactor with a fixed bed catalyst. Experiments were performed at 450–600 $^\circ\text{C}$, atmospheric pressure, a rapeseed oil space velocity of 3.1 h^{-1} and at time on stream (TOS) of 2 h. Hydrogen was fed into the reactor along

with rapeseed oil at a rate of 2 $\text{dm}^3 \text{ h}^{-1}$ to suppress coking. The detailed procedure of the catalytic experiments and the data on the composition of liquid organic products of rapeseed oil conversion was determined by GLC and FTIR spectroscopy (see Online Supplementary Materials).

In all experiments at 450–600 $^\circ\text{C}$, close to 100% conversion of rapeseed oil was achieved, as proved by FTIR spectroscopy. Figure 1 shows the IR spectra of (a) rapeseed oil and (b) a liquid organic product obtained at 450 $^\circ\text{C}$. The IR spectrum of rapeseed oil exhibits absorption bands typical for the functional groups of esters (1743 and 1159 cm^{-1}) and saturated and unsaturated alkanes (2852 and 3007 cm^{-1}). Absence in the IR spectrum of the liquid organic product of absorption bands of carbonyl groups at 1742–1744 cm^{-1} and bands of stretching vibrations of CO bonds of higher carboxylic acid esters at 1159–1162 cm^{-1} which are characteristic of rapeseed oil,¹⁹ confirms 100% conversion of rapeseed oil. Absorption bands at 1743 cm^{-1} (C=O) and 1159 cm^{-1} (C–O) were also absent in the liquid organic products obtained by rapeseed oil conversion at 500–600 $^\circ\text{C}$. At the same time, the IR spectrum of the liquid organic product formed at 450 $^\circ\text{C}$ shows the absorption band at 1709 cm^{-1} typical for the carbonyl group C=O of carboxylic acids.¹⁹ This means that the complete conversion of the fatty acids intermediates has not been achieved at this temperature.

The IR spectra of the products obtained at 500–600 $^\circ\text{C}$ is presented in Figures S2–S4. In the IR spectra of these products, the absorption band at 1709 cm^{-1} characteristic of the C=O carbonyl group was no longer present. In addition, in the IR spectra of the liquid organic products obtained at 500 and 550 $^\circ\text{C}$, there were no absorption bands of OH groups in the range of 3400–3500 cm^{-1} . Consequently, the complete conversion of oxygen-containing intermediates derived from rapeseed oil into hydrocarbons over the HMFI/SiC catalyst was reached at 500–600 $^\circ\text{C}$.

The IR spectra of the liquid organic products obtained at different temperatures show the absorption band at 728 cm^{-1} corresponding to the out-of-plane bending vibrations of CH_2 -groups of *n*-alkanes and/or olefins, as well as the absorption band at 3007 cm^{-1} , which corresponds to the stretching vibrations of C–H bonds. The presence of absorption bands in the range of 909–675 cm^{-1} in the spectra indicates that aromatic hydrocarbons are contained in the products.^{19–21} Products yields observed in

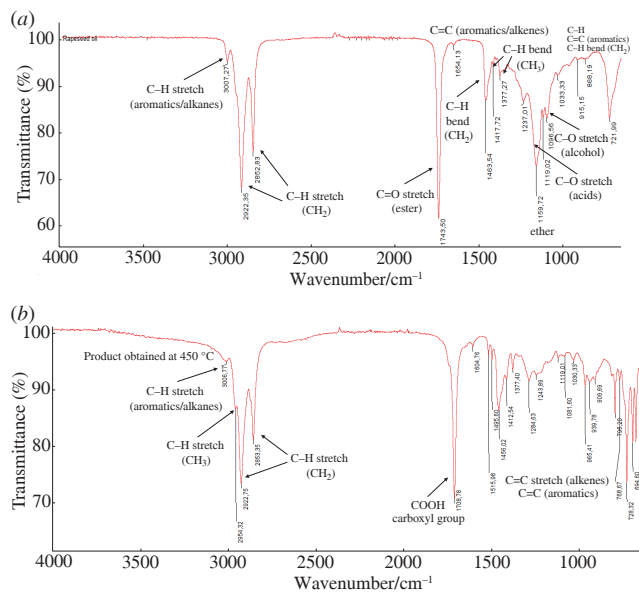


Figure 1 Comparative FTIR analysis of (a) rapeseed oil and (b) the liquid organic product of rapeseed oil conversion catalyzed by HMFI/SiC at 450 $^\circ\text{C}$ in H_2 flow.

catalytic conversion of rapeseed oil at 450 °C are presented in the Table S4. The results obtained on a freshly prepared catalyst, a catalyst not subjected to oxidative regeneration and a catalyst after oxidative regeneration are shown. The data prove that the non-regenerated catalyst dramatically reduces the yield of BTX fraction. At the same time, the catalyst after oxidative regeneration demonstrates results similar to those obtained on a freshly prepared catalyst. Table S4 also displays the examples of mass balance closure, inasmuch as the conversion rate was 100%. The gaseous products contain traces of CO, CO₂ and H₂O that, according to,²¹ result from the conversion of fatty acid triglycerides. The liquid organic products predominantly contain aromatics, as well as C₅₊, including olefins, paraffins, iso-paraffins and cycloparaffins.

Table 1 illustrates the effect of temperature on the total yields of the liquid organic products, aromatics and *p*-xylene produced by rapeseed oil conversion over the HMFI/SiC, as well as the content of *p*-xylene in the mixture of the isomeric xylenes.

As is seen from Table 1, when the temperature rises from 450 to 600 °C the yield of the liquid organic products decreases from 61 to 28 wt%; in particular, the total yield of aromatic hydrocarbons decreases from 39 to 19 wt%. It is worth noting that in the experiment run at 450 °C a higher total yield of arenes is observed, the yield of *p*-xylene reaches 6 wt%, its content in the mixture of isomeric xylenes is 75 wt%. An increase in temperature from 450 to 600 °C results in the decrease in *p*-xylene content in the mixture of isomers.

Thus, achievement of a higher yield of *p*-xylene and its larger content in the mixture of isomeric xylenes and liquid organic products is promoted by running rapeseed oil conversion over the HMFI/SiC catalyst at 450–500 °C.

Figure 2 shows the data of TEM for the spent HMFI/SiC catalyst after oxidative regeneration. It is noteworthy that the sample was studied on a carbon-containing grid; therefore, carbon was not analyzed. The micrographs on Figures 2(a), (b) show zeolite particles decorated with the amorphous phase of silicon carbide. The EDX elemental mappings of the composite [Figures 2(c)–(f)] show that oxygen is predominately located in zeolite particles, while silicon is uniformly distributed over silicon carbide and zeolite. The presence of oxygen in the silicon carbide phase can be associated with SiO₂ and SiO_xC_y formation during oxidative regeneration of the catalyst.²²

The amount of coke deposited on the spent, unregenerated catalyst was assessed by thermogravimetric analysis. According to Figure 3, for the spent catalyst heated in an air flow, the weight loss of 5% in the temperature range of 400–650 °C, that corresponds to the combustion of coke of an ordered polycyclic nature.²³

Comparison of the literature data on the synthesis of *p*-xylene from biogenic feedstocks over catalysts containing non-promoted zeolites ZSM-5 with the results of this study is given in Table S5. In the conversion of jatropha oil¹⁸ and fatty acids²⁴ on the ZSM-5 at 450 °C at atmospheric pressure the content of *p*-xylene in the mixture of isomeric xylenes reached 50 and 57%, respectively. For comparison, the data on *p*-xylene production by toluene disproportionation over ZSM-5 zeolite under comparable conditions are presented.²⁵ The data of Table S5 show that when

Table 1 Effect of temperature on the yield of selected products of rapeseed oil conversion.

Products	Yield (wt%)			
	450 °C	500 °C	550 °C	600 °C
Liquid organic products	61	50	37	28
Aromatics	39	29	24	19
<i>p</i> -Xylene	6 (75) ^a	5 (70) ^a	4 (67) ^a	2 (62) ^a

^aContent of *p*-xylene in the mixture of isomeric xylenes (wt%).

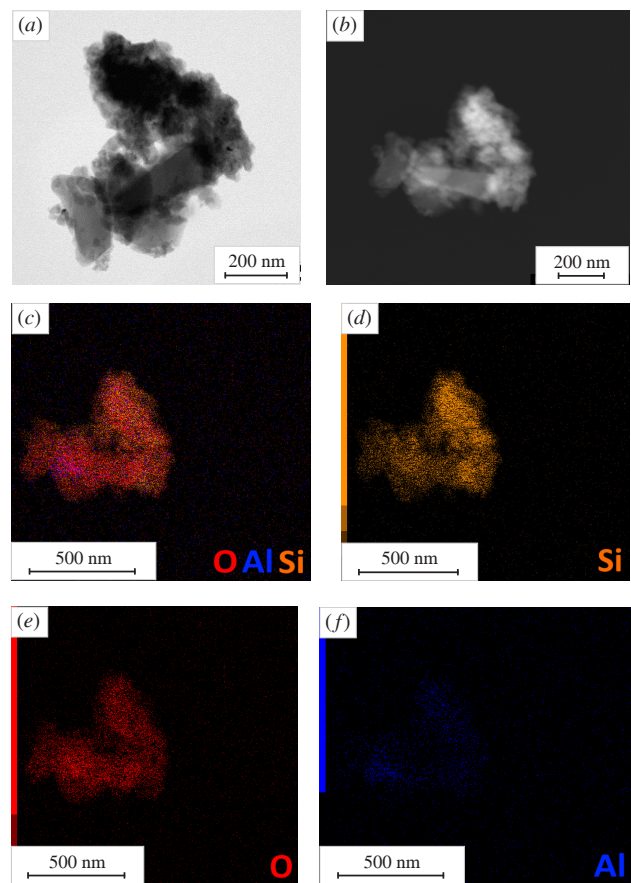


Figure 2 (a) TEM and (b) STEM images and (c)–(f) EDX elemental mappings of the spent HMFI/SiC after regeneration.

using the HMFI/SiC catalyst, the product with a high *p*-xylene content in the mixture of the isomeric xylenes can be obtained from the biogenic feedstock (rapeseed oil).

To sum up, it has been shown for the first time that the HMFI/SiC catalytic material synthesized by the hydrothermal microwave method catalyzes the conversion of rapeseed oil into liquid hydrocarbons. In this case, *p*-xylene predominates among the isomeric xylenes contained in the resulting hydrocarbons. It has been demonstrated that the rapeseed oil conversion at 450 °C produced, TOS 2 h and hydrogen supply to the reactor allowed us to obtain *p*-xylene with a yield up to 6 wt%, with its content in the mixture of isomeric xylenes being as high as 75 wt%. Oxidative regeneration of the spent catalyst after the reaction carried out for 2 h makes it possible to achieve a reproducible yield of *p*-xylene. The process has the following advantages: *p*-xylene is produced from the renewable feedstock, the reaction is run at the atmospheric pressure and the catalyst containing no noble metals is used.

This research was carried out within the state funding of TIPS RAS.

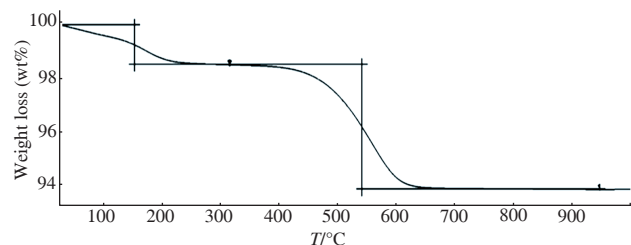


Figure 3 Thermogravimetric analysis of the spent HMFI/SiC catalyst.

Online Supplementary Materials

Supplementary data associated with this article can be found in the online version at doi: 10.71267/mencom.7625.

References

- 1 S. Z. Naji, C. Y. Tye and A. A. Abd, *Process Biochem.*, 2021, **109**, 148; <https://doi.org/10.1016/j.procbio.2021.06.020>.
- 2 Z. Zhang, X. Xie, W. J. Lee, G. Zhao, C. Li and Y. Wang, *Food Chem.*, 2022, **371**, 131177; <https://doi.org/10.1016/j.foodchem.2021.131177>.
- 3 A. F. Lee, J. A. Bennett, J. C. Manayil and K. Wilson, *Chem. Soc. Rev.*, 2014, **43**, 7887; <https://doi.org/10.1039/C4CS00189C>.
- 4 P. Arora, H. Abdolahi, Y. W. Cheah, M. A. Salam, E. L. Grennfelt, H. Rådberg, D. Creaser and L. Olsson, *Catal. Today*, 2021, **367**, 28; <https://doi.org/10.1016/j.cattod.2020.10.026>.
- 5 N. A. Negm, A. M. Rabie and E. A. Mohammed, *Appl. Catal., B*, 2018, **239**, 36; <https://doi.org/10.1016/j.apcatb.2018.07.070>.
- 6 N. Le-Phuc, T. V. Tran, T. T. Phan, P. T. Ngo, Q. L. M. Ha, T. N. Luong, T. H. Tran and T. T. Phan, *J. Renew. Energy*, 2021, **168**, 57; <https://doi.org/10.1016/j.renene.2020.12.050>.
- 7 E. David, *Appl. Catal., A*, 2021, **617**, 118126; <https://doi.org/10.1016/j.apcata.2021.118126>.
- 8 A. Galadima and O. Muraza, *J. Ind. Eng. Chem.*, 2015, **29**, 12; <https://doi.org/10.1016/j.jiec.2015.03.030>.
- 9 M. Albahar, C. Li, V. L. Zholobenko and A. A. Garforth, *Microporous Mesoporous Mater.*, 2020, **302**, 110221; <https://doi.org/10.1016/j.micromeso.2020.110221>.
- 10 X. Huang, R. Wang, X. Pan, C. Wang, M. Fan, Yu. Zhu, Y. Wang and J. Peng, *Green Energy Environ.*, 2020, **5**, 385; <https://doi.org/10.1016/j.gee.2019.12.001>.
- 11 A. G. Dedov, A. S. Loktev, E. A. Isaeva, A. A. Karavaev, Yu. N. Kitashov, S. V. Markin, A. E. Baranchikov, V. K. Ivanov and I. I. Moiseev, *Pet. Chem.*, 2017, **57**, 415; <https://doi.org/10.1134/S0965544117080035>.
- 12 A. G. Dedov, A. S. Loktev, A. A. Karavaev and I. I. Moiseev, *Mendeleev Commun.*, 2018, **28**, 352; <https://doi.org/10.1016/j.mencom.2018.07.002>.
- 13 S. M. Sadrameli, A. E. S. Green and W. Seames, *J. Anal. Appl. Pyrolysis*, 2009, **86**, 1; <https://doi.org/10.1016/j.jaap.2008.02.004>.
- 14 A. G. Dedov, A. A. Karavaev, A. S. Loktev and M. N. Vagapova, *Patent RU 2806584*, 2023; <https://patents.google.com/patent/RU2806584C1/ru>.
- 15 A. G. Dedov, A. S. Loktev, A. A. Karavaev, A. S. Mitinenko, E. A. Isaeva and I. I. Moiseev, *Patent RU 2725586*, 2020; <https://patents.google.com/patent/RU2725586C1/ru>.
- 16 A. G. Dedov, A. A. Karavaev, A. S. Loktev, A. S. Mitinenko, K. A. Cherednichenko and I. I. Moiseev, *Mater. Lett.*, 2021, **290**, 129497; <https://doi.org/10.1016/j.matlet.2021.129497>.
- 17 A. G. Dedov, A. A. Karavaev, A. S. Loktev, P. V. Zemlianskii, M. N. Vagapova, K. I. Maslakov, K. A. Cherednichenko, S. V. Egazar'yants, A. V. Khoroshilov and P. I. Ivanov, *Mendeleev Commun.*, 2023, **33**, 832; <https://doi.org/10.1016/j.mencom.2023.10.031>.
- 18 O. Singh, A. Agrawal, N. Dhiman, B. P. Vempatapu, K. Chiang, S. Tripathi and B. Sarkar, *Renew. Energy*, 2021, **179**, 2124; <https://doi.org/10.1016/j.renene.2021.08.011>.
- 19 F. Pinto, S. Martins, M. Gonçalves, P. Costa, I. Gulyurtlu, A. Alves and B. Mendes, *Appl. Energy*, 2013, **102**, 272; <https://doi.org/10.1016/j.apenergy.2012.04.008>.
- 20 L. N. S. Freitas, F. P. de Sousa, A. R. de Carvalho and V. M. D. Pasa, *Fuel*, 2021, **287**, 119472; <https://doi.org/10.1016/j.fuel.2020.119472>.
- 21 V. P. Doronin, O. V. Potapenko, P. V. Lipin, T. P. Sorokina and L. A. Bulachevskaya, *Pet. Chem.*, 2012, **52**, 422; <https://doi.org/10.1134/S0965544112060059>.
- 22 Y. Liu, S. Podila, D. L. Nguen, D. Edouard, P. Nguen, C. Pham, M. J. Ledoux and C. Pham-Huu, *Appl. Catal., A*, 2011, **409–410**, 113; <https://doi.org/10.1016/j.apcata.2011.09.035>.
- 23 J. A. Botas, D. P. Serrano, A. García and R. Ramos, *Appl. Catal., B*, 2014, **145**, 205; <https://doi.org/10.1016/j.apcatb.2012.12.023>.
- 24 R. Hilten, R. Speir, J. Kastner and K. C. Das, *Bioresour. Technol.*, 2011, **102**, 8288; <https://doi.org/10.1016/j.biortech.2011.06.049>.
- 25 E. E. Knyazeva, S. V. Konnov, A. A. Tikhonova, O. A. Ponomareva and I. I. Ivanova, *Pet. Chem.*, 2015, **55**, 500; <https://doi.org/10.1134/S0965544115080149>.

Received: 18th September 2024; Com. 24/7625